Applied Energy Symposium 2020: Low carbon cities and urban energy systems
October 10-17, 2020
Paper ID: CUE2020-D-097

Influence of operation parameters on heat extraction performance of dry hot rock

Jianxiao Zhu[1,2], Xueling Liu[*1,2] ,Yuanming Wang[1,2]
1 Key Laboratory of Efficient Utilization of Low and Medium Grade Energy, MOE, Tianjin University, Tianjin, 300354, China
2 Geothermal Research &Training Center, Tianjin University, Tianjin, 300354, China
Corresponding author: lxling@tju.edu.cn

ABSTRACT

Due to the superior hydrothermal properties and CO_2 geological storage, Super-critical carbon dioxide ($ScCO_2$) has superior performance as working fluid in Enhanced geothermal system (EGS). In this paper, a three-dimensional fracture grid model is established to obtain the flow and heat transfer characteristics of $ScCO_2$ in Hot dry rock (HDR). The influence of mass flow rate on heat extraction performance and flow characteristics in EGS is evaluated, and outlet temperature and flow resistance with operation time is obtained. The results indicate that the fluid temperature of production well begins to decrease when heat extraction operates two years. The greater the mass flow rate, the greater the decline speed and range. After ten years of operation, the maximum drop of the fluid temperature of production well is 65 K. With the increase of mass flow rate, the heat extraction capacity increases, the heat extraction of unit mass flow $ScCO_2$ decreases, and both of them decrease with operation time. With the increase of mass flow rate, the flow resistance increases, which causes larger consumption of circulation pump power. In addition, the power consumption per unit heat extraction increase.

Keywords: EGS, heat transfer, flow resistance, super-critical carbon dioxide

1. INTRODUCTION

As a kind of geothermal energy, HDR has great development potential [1-4]. EGS is an important means to develop and utilize HDR [5]. In 2000, CO_2-based geothermal system was proposed for the first time, and was found to have significant advantages [6] [7]. Cao [8] found that $ScCO_2$-based EGS has higher mass flow rate and higher heat release rate than the EGS with water as working fluid, but its service life was shorter. Atrens[9] pointed out that thermal siphon can be used to drive $ScCO_2$ to reduce the degree of fouling dissolution. Yun Chen et al. [10] estimated the fluid outlet temperature better based on the local non thermal equilibrium theory(LNTE). Zhang J et al. [11] established a tree shaped well model with lower flow resistance and higher extraction rate. Chen and Jiang [12] studied the influence of multi well layout on the thermal extraction performance of EGS based on homogeneous single pore model, and found that three well triangle layout had the best thermal extraction performance. Garipov and Hui [13] found that the injected fluid can significantly change the reservoir structure, resulting in fracture surface slip and the increase of permeability. Yao et al. [14] found that Darcy's law can be used to calculate fluid flow in fractures. With the increase of fracture size, the flow rate first increases slowly and then increases sharply. At present, there is still a gap in the long-term operation of $ScCO_2$-based EGS. The heat transfer process of $ScCO_2$ in HDR is investigated in present work.

2. PHYSICAL MODEL

The fracture in the HDR energy storage system was the fractured porous medium constructed by artificial fracturing [15]. In this paper, Monte Carlo method [15] is used to establish fracture grid. The main core parameters of fractures are center point, inclination, dip angle and trace length. In the process of fracture construction, the center point of fracture is uniformly distributed, the dip angle and inclination of fracture surface conform to normal distribution or lognormal distribution, and trace length follows exponential distribution or lognormal distribution. The average trace length is 70 m, the variance is 30, and the average inclination and dip angle

Selection and peer-review under responsibility of the scientific committee of CUE2020

are 0 °. Two wells with a spacing of 300 m and a height of 500 m are set up, which are inlet well and outlet well respectively. The permeable reservoir is a cube 500m long on each side while surrounding rock's is 800m. The horizontal plane of reservoir central height is the main channel fracture. The structure of heat extraction system in HDR is shown in Fig 1. The parameters of EGS is shown in Table 1.

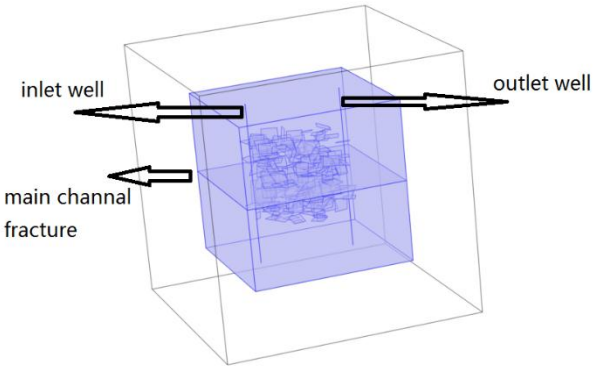

Fig 1 Structure of EGS

Table 1 Parameters of EGS

Parameter	value
Density of rock matrix :ρ_p(kg/m^3)	2700
Specific heat capacity of rock matrix at constant pressure :Cp,p(J/(kg•K))	1000
Thermal conductivity of rock matrix :k_p(W/(m•K))	3.0
Porosity of rock matrix :ε_p	0.01
Permeability of rock matrix: κ(m^2)	10^{-15}
Fracture thickness :d_f(m)	0.001
Injection temperature of dry hot rock of injection well : T_{inj}	70
Surface environmental temperature :T_{sur}(° C)	20
Surface environmental pressure: P_{sur}(MPa)	0.1
Ground temperature gradient: dt/dz(° C/m)	0.04
Ground pressure gradient: dp/dz(MPa/m)	0.008

3. MATHEMATICAL MODEL

In the numerical process, it is assumed that the rock is a continuous porous medium and isotropic, and the permeability of the rock matrix is much lower than that of the fracture. There is no mass loss in the flow of heat carrying fluid in the fracture and in the rock matrix, and flow in fracture porous medium obey Darcy's law. Thermal stress caused by temperature change and its influence on the physical properties of rock matrix and fracture are ignored. Chemical reaction between rock matrix and fluid is ignored as well.

3.1 governing equations

The continuity equation of working fluid is as follows

$$\frac{\partial}{\partial t}\left(\varepsilon_p \rho\right)+\nabla\cdot\left(\rho\mathbf{u}\right)=Q_m \qquad (3\text{-}1)$$

Where, ε_p is the porosity of the rock matrix; ρ is the fluid density, kg/m^3; **u** is the seepage velocity of the fluid in the rock matrix, m/s; Q_m is the mass source term, kg/(m^3/s); here it refers to the charged and discharged fluid.

According to Darcy's law, flow velocity of working fluid in dry hot rock fracture is:

$$\mathbf{u}=-\frac{\kappa}{\mu}\left(\nabla p+\rho\mathbf{g}\right) \qquad (3\text{-}2)$$

Where, κ is the permeability of rock matrix; g is the acceleration of gravity, m/s^2.

Momentum equation of working fluid is:

$$\rho\left(\frac{\delta\mathbf{u}}{\delta\tau}+\left(\mathbf{u}\cdot\nabla\right)\mathbf{u}\right)=-\nabla P+\mu\cdot\nabla^2\mathbf{u} \qquad (3\text{-}3)$$

Where P is the fluid pressure, Pa; μ is the hydrodynamic viscosity, Pa·s.

The energy equation in EGS is as follows，

$$(\rho c)_{eff}\frac{\delta T_s}{\delta\tau}+(\rho c)_{eff}\,\mathbf{u}_s\cdot\nabla T_s=\nabla(\lambda_{eff}\nabla T_s) \qquad (3\text{-}4)$$

Where, $(\rho c)_{eff}$ is the equivalent volume heat capacity of the fractured porous medium, J/m^3·K; λ_{eff} is the equivalent thermal conductivity coefficient, W/ (m ·K).

$$(\rho c)_{eff}=(1-\varphi_s)\rho_s c_s+\varphi_s\rho c \qquad (3\text{-}5)$$

$$\lambda_{eff}=(1-\varphi_s)\lambda_s+\varphi_s\lambda \qquad (3\text{-}6)$$

Among them, the subscript of s indicates the physical properties of rock matrix, and the others are the physical properties of fluid , Φ_s is the porosity of rock matrix.

3.2 boundary and initial conditions

The boundary conditions of the computational domain are as follows:

The thermal boundary condition of surrounding rock is adiabatic:

$$\frac{\delta T}{\delta n}\cdot\vec{n}=0 \qquad (3\text{-}7)$$

Where $\vec{n}$ is the unit normal vector of the interface.

The flow boundary condition of permeable reservoir is no flow boundary:

$$-\mathbf{n}\cdot\rho\mathbf{u}=0 \quad (3\text{-}8)$$

The temperature and pressure of the injection well:

$$T=T_{inj},P=P_{inj} \quad (3\text{-}9)$$

Pressure of production well:

$$P=P_{pro} \quad (3\text{-}10)$$

In computational domain, the initial conditions of rock matrix and fracture network are as follows:

Pressure:

$$P=dP/dz\cdot abs(z) \quad (3\text{-}11)$$

Temperature:

$$T=453.15\,K+(abs(z)-4000\,m)\cdot dT/dz \quad (3\text{-}12)$$

Where abs(Z) is absolute value of depth.

3.3 Numerical method

In present work, COMSOL Multiphysics is used for numerical simulation. The maximum time step size is 60 days, the maximum BDF order is 2 order, the minimum BDF order is 1, the tolerance is 0.01, the residual tolerance is 0.01, and the maximum number of iterations is 10000. The physical field obeys Darcy's law, fracture flow, porous media heat transfer and fracture heat transfer coupling. Darcy's law and fracture flow are pressure quadratic discretization, and porous media heat transfer and fracture heat transfer are discretized by temperature as linear unit.

3.4 Grid independence verification

In order to verify the accuracy of the numerical results and the cost of the numerical simulation, the independence test of the grid is performed. Outlet well temperature is obtained under the grid number of 1.25 million, 1.55 million, 1.75 million and 2 million.

Table 2 Outlet temperature under different grid numbers

Number of grids (million)	outlet temperature（K）
1.25	421.0236
1.55	429.2164
1.75	431.2216
2.00	431.5324

$$\varepsilon_{155,125}=T_{155}-T_{125}=8.19K$$
$$\varepsilon_{175,155}=T_{175}-T_{155}=2.0052K$$
$$\varepsilon_{200,175}=T_{200}-T_{175}=0.3160K$$

$$R_{125,155,175}=\frac{\varepsilon_{175,155}}{\varepsilon_{155,125}}=0.2448$$

$$R_{155,175,200}=\frac{\varepsilon_{200,175}}{\varepsilon_{175,155}}=0.1576$$

$$0<R_{155,175,200}<R_{125,155,175}<1$$

According to Richardson extrapolation method [16], it can be considered that the convergence condition is satisfied when R < 1. In order to ensure the accuracy of calculation and reduce the cost of numerical simulation, 1.55 million grids were selected.

4. MODEL ACCURACY EVALUATION

To evaluate accuracy of present model, results are compared with the results in the literature [17]. The computational domain is a cuboid whose size is 1000×1000×200m , and its depth is 3000-3200m. The length of injection and production wells is 50m, and distance between them is 350m. The mass flow rate of injection well is 100kg/day and the pressure of production well is 20 MPa. Temperature of injection fluid is 293 K and geothermal gradient is 0.05K/m. The comparison is shown in Fig 2. Numerical results in this model is represented as N-results, and the results in the literature is represented as R-results.

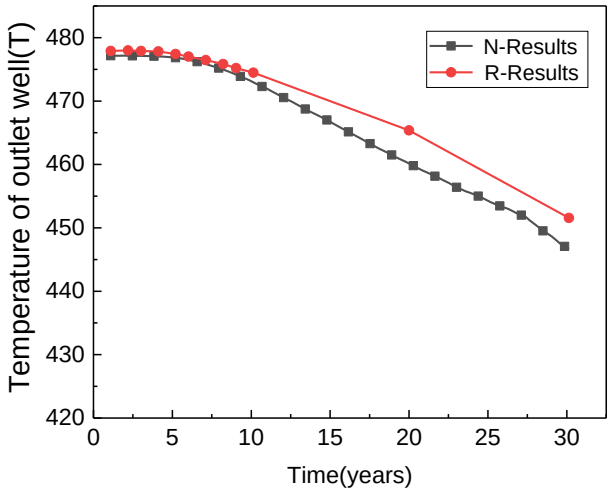

Fig 2 Model accuracy evaluation

The maximum difference of outlet temperatures between the two results is about 6 K which happens on 20th years, error is about 1.2%. So present model is accurate and reliable.

5. RESULTS AND DSICUSSION

5.1 heat transfer characteristics

In order to probe the influence of operating parameters on heat extraction of $ScCO_2$-based EGS, when inlet temperature of working medium is 70℃, the variation of outlet temperature of production well, heat extraction and power consumption of circulating pump under different mass flow rates are obtained.

When mass flow rates are 33 kg/s, 40 kg/s, 45 kg/s and 55 kg/s, the variation of outlet temperature of production well with time is shown in Fig 3.

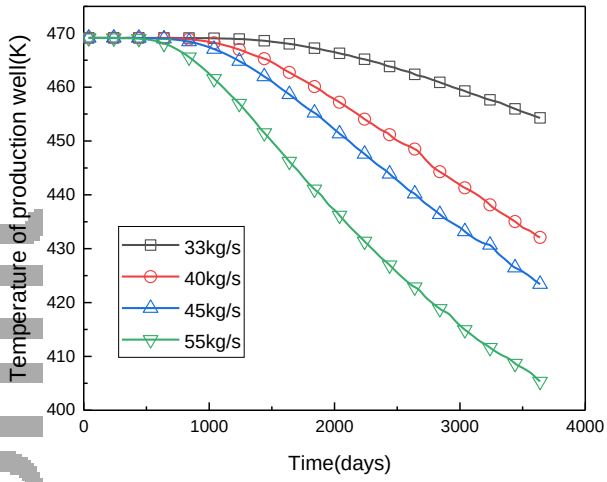

Fig 3 Production temperature under different mass flow rates and time

It can be seen from Fig 3 that under each mass flow rate, the fluid temperature of production well begins to decrease after two-year operation. The greater the flow rate, the greater the temperature attenuation rate and amplitude. When the mass flow rates are 33 kg/s, 40 kg/s and 45 kg/s, the temperature of production well drops are 15 K, 40 K and 45 K respectively. When mass flow rate is 55 kg/s, the largest temperature drop is about 65 K. It's because that heat extraction capacity of working fluid is stronger than thermal compensation of surrounding rock, causing the temperature drop of rock matrix in reservoir.

Fig 4 shows the total heat extraction of working fluid under different mass flow rates. The greater the mass flow rate, the greater the heat extraction quantity. With the running of this system, quantity of heat extraction gradually decreases. It decreases more obviously under the condition of larger mass flow rate. During the ten years, when the mass flow rates are 33 kg/s, 40 kg/s and 45 kg/s, the heat extraction rates decrease 4%, 9% and 11% respectively. When the mass flow rate is 55 kg/s, the heat extraction decreases about 16%.

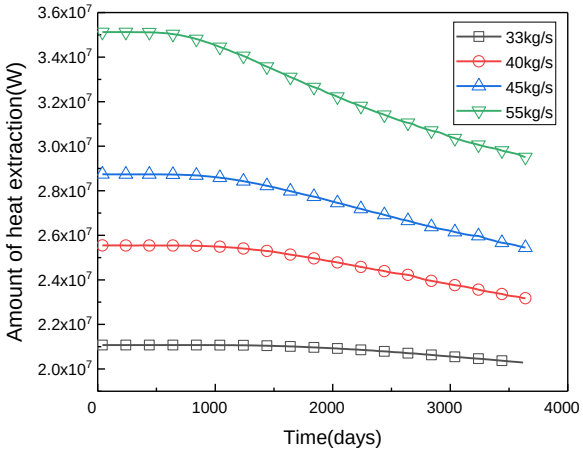

Fig 4 Heat extraction under different mass flow rates

Heat extraction of working fluid per unit mass flow under different mass flow rates is shown in Fig 5. The higher the mass flow rate, the smaller the heat extraction per unit mass flow rate. And with the running of system, heat extraction per unit mass of working fluid gradually decreases, and the greater the mass flow rate, the more obvious the decrease. When the mass flow rates are 33 kg / s, 40 kg / s and 45 kg / s, the decrease ratio are 3%, 9% and 11% respectively. When the mass flow rate is 55 kg / s, the biggest decrease ratio is 16%.

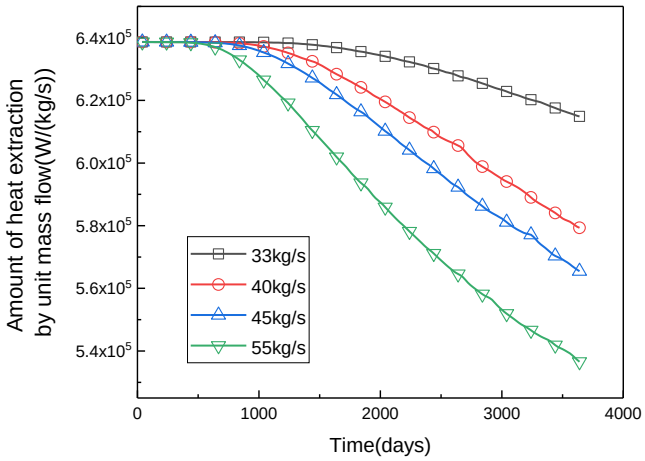

Fig 5 Heat extraction per unit mass flow rate

5.2 flow characteristics of working fluid

Fig 6 shows flow resistance of fluid and total power consumption of circulating pump with different mass flow rates in HDR.

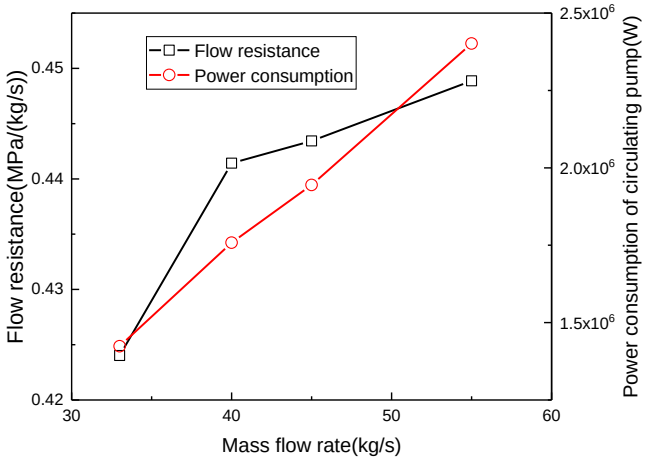

Fig 6 Flow resistance and power consumption of circulating pump under different mass flow rate

Fig 6 shows that the larger the mass flow rate, the greater the flow resistance and total power consumption of circulating pump. When the mass flow rates are 33 kg/s, 40 kg/s, 45 kg/s and 55 kg/s, the flow resistance are 0.424 MPa/(kg/s)), 0.441 MPa/(kg/s)), 0.443 MPa/(kg/s)) and 0.448 MPa/(kg/s)) respectively, total power consumptions are 1.42×10^6 W, 1.76×10^6 W, 1.94×10^6 W and 2.40×10^5 W.

Table 3 shows the relationship between mass flow rate and ratio of power consumption of circulating pump and heat extraction ($Ratio_{p,q}$).

Table 3 $Ratio_{p,q}$ under different mass flow rate

Mass flow rate(kg/s)	$Ratio_{p,q}$
33	0.06755
40	0.06767
45	0.06837
55	0.06883

Table 3 shows : With the increase of mass flow rate, the power consumption by unit heat extraction increase.

6. CONCLUSION

In present work, the flow and heat transfer characteristics are obtained when $ScCO_2$ is used as working fluid in HDR. The main conclusions are as following:

(1) When the system has been running for about two years, the outlet temperature of the working medium will be attenuated, and the greater the mass flow rate, the faster the attenuation speed and the greater the attenuation degree. When the mass flow rate is 55 kg / s, the outlet temperature drops by about 65 K after ten years of operation.

(2) The higher the mass flow rate, the greater the total heat extraction of working medium, and the smaller the heat extraction per unit mass of working medium. With the running of system, the total heat extraction and heat extraction per unit mass flow rate decrease under each mass flow rate, and the larger the mass flow rate, the greater the decrease range.

(3) The greater the mass flow rate, the greater the flow resistance, the greater total power consumption of circulating pump and power consumption per unit heat extraction.

ACKNOWLEDGEMENT

The authors gratefully acknowledge the financial support provided by the Natural Science Foundation of Tianjin (No.18JCYBJC22100).

REFERENCE

[1] Petroleum B. BP Statistical Review of World Energy - June 2010 [J]. Economic Policy, 2011, 4: 38-55.

[2] Bahadori A, Zendehboudi S, Zahedi G. A review of geothermal energy resources in Australia: Current status and prospects [J]. Renewable and Sustainable Energy Reviews, 2013, 21: 29-34.

[3] Li K, Bian H, Liu C, et al. Comparison of geothermal with solar and wind power generation systems [J]. Renewable and Sustainable Energy Reviews, 2015, 42:1464-1474.

[4] Bertani R. Geothermal power generation in the world 2005–2010 update report [J]. Geothermics, 2012, 41: 1-29.

[5] Lu S. A global review of enhanced geothermal system (EGS) [J]. Renewable and Sustainable Energy Reviews 2018, 81: 2902–2921.

[6] Brown D W. A hot dry rock geothermal energy concept utilizing supercritical CO_2 instead of water [C]. Proceedings Twenty-fifth Workshop Geothermal Reservoir Engineering 2000, Stanford, California: Stanford University, 2000: 233-238.

[7] Pruess K. Enhanced geothermal systems (EGS) using CO_2 as working fluid—A novel approach for generating renewable energy with simultaneous sequestration of carbon [J]. Geothermics, 2006, 35(4): 351-367.

[8] Cao W, Huang W , Jiang F. Numerical study on variable thermophysical properties of heat transfer fluid affecting EGS heat extraction [J]. International Journal of Heat and Mass Transfer, 2016, 92: 1205-1217.

[9] Atrens AD, Gurgenci H, Rudolph V. Electricity generation using a carbon-dioxide thermosiphon. Geothermics. 39(2): p. 161-169.14
[10] Chen Y, Ma G, Wang H. Heat extraction mechanism in a geothermal reservoir with rough-walled fracture networks[J]. International Journal of Heat and Mass Transfer,2018,126.
[11] Zhang J, Xie J, Liu X. Numerical evaluation of heat extraction for EGS with tree-shaped wells[J]. International Journal of Heat and Mass Transfer, 2019, 134:296-310.
[12] Chen J, Jiang F. Designing multi-well layout for enhanced geothermal system to better exploit hot dry rock geothermal energy [J]. Renewable Energy, 2015, 74: 37-48.
[13] Garipov T T, Hui M. Discrete Fracture Modeling approach for simulating coupled thermo-hydro-mechanical effects in fractured reservoirs [J]. International Journal of Rock Mechanics and Mining Sciences, 2019, 122: 104075.
[14] Yao W, Sharifzadeh M, Yang Z, et al. Assessment of fracture characteristics controlling fluid flow performance in discrete fracture networks (DFN) [J]. Journal of Petroleum Science and Engineering, 2019, 178: 1104-1111.
[15] Huang Z, Yao J, Wang Y, Tao K. Numerical study on two-phase flow through fractured porous media[J]. Science China Technological Sciences,2011,54(9).
[16] Wang J, Jiao Y, Liu X. Heat transfer and flow characteristics in a rectangular channel with small scale vortex generators[J]. International Journal of Heat and Mass Transfer,2019,138.
[17] Guo T, Gong F, Wang X, Lin Q, Qu Z, Zhang W. Performance of enhanced geothermal system (EGS) in fractured geothermal reservoirs with CO_2 as working fluid. Applied Thermal Engineering. 2019;152.